J. Fluid Mech. (1972), *vol.* 56, *part* 2, *pp.* 353–374
Printed in Great Britain

Finite amplitude doubly diffusive convection

By JOE M. STRAUS

Department of Planetary and Space Science,
University of California, Los Angeles

(Received 19 April 1972)

A layer of fluid containing gradients of both temperature and salinity is subject to several instabilities of geophysical interest. When the salinity and temperature increase upwards, the layer may become unstable even if the density profile indicates stability. This 'doubly diffusive' instability, first treated by Stern, is seen experimentally to consist of thin fingers of up- and downgoing fluid. Linear analysis cannot explain this small horizontal scale for a steady-state process, but a nonlinear treatment of the problem combined with a stability analysis indicates that only small-scale motions are stable when the salinity gradient is larger than that necessary for the onset of instability. In the limit of small salt diffusivity the flux of salt is calculated using the Galerkin technique and found to reach a maximum at a wavelength that decreases with increasing salinity and temperature gradients. The stability of the finite amplitude solutions is treated; only small-scale motions are found to be stable and the wavelength of the most stable mode is found to compare favourably with the wavelength that maximizes the salt flux.

1. Introduction

There has been considerable interest recently in a class of hydrodynamic instabilities that has come to be called 'doubly diffusive'. This type of instability, which may arise even when the fluid is stably stratified, depends for its driving mechanism on the different diffusive properties associated with two forces, one of which is stabilizing, one destabilizing. This is to be contrasted with singly diffusive instabilities, in which there is no stabilizing component (other than dissipation). Typical representatives of doubly diffusive instabilities are the salt finger instability, first treated by Stern (1960), and an instability associated with differential rotation in stars, treated by Goldreich & Schubert (1967). The salt finger instability can arise in a horizontal layer of fluid in which gradients of both temperature and salinity are positive upwards. Because salt diffuses at a much slower rate than does heat, a parcel of fluid perturbed downwards loses its stabilizing temperature excess so much faster than its destabilizing salinity excess that it can continue downwards even if the initial density profile was a stable one. The doubly diffusive character of the salt finger instability is clear: both temperature and salinity influence the density of the fluid, and the instability requires that the stabilizing quantity (temperature) diffuses more rapidly than the destabilizing one (salinity). The instability of differentially rotating stars involves

an unstable angular momentum distribution (decreasing outwards) and a subadiabatic temperature profile, corresponding to stable stratification. Instability can occur because, in the radiative zone of a star, momentum diffuses much less rapidly than heat. On being perturbed, a parcel of fluid comes into thermal equilibrium with its surroundings much more rapidly than its angular momentum can equilibrate, so that instability can result.

In laboratory experiments the salt finger instability is always seen to set in as thin cells of fluid moving alternately up and down in the stably stratified layer. Stern (1960) suggests that the experimentally observed structure is due to the fact that the fastest-growing mode is the one which will dominate. He has shown that, when the salinity gradient is greatly in excess of the value necessary for the onset of instability, the mode which maximizes the growth rate of infinitesimal perturbations has a much smaller scale than that at marginal stability. In the same way, Goldreich & Schubert found that thin cells maximize the growth rate of infinitesimal disturbances in a region of unstable angular momentum gradient in stars, and thus predict a similar structure in that situation.

In a steady-state process, with the value of the relevant parameters well above those necessary for the onset of instability, however, linear theory cannot be called upon to explain the horizontal scale of the motion. Linear theory leaves the amplitude of the motion undetermined, predicts that unstable modes grow exponentially in time and provides no mechanism for the flow to reach a steady state. As the amplitude of the motion increases, interactions of finite amplitude modes with each other become important and cannot be disregarded in a treatment of the problem. Thus nonlinear effects must be included if any accurate analysis of the properties of the steady-state system is desired. It is such an analysis that will be carried out here. The two major goals of this paper are: first, a clarification of the wavelength question in doubly diffusive instabilities; and second, an evaluation of the effectiveness of doubly diffusive instabilities in the transport process. In discussing these two major topics, the salt finger instability will be treated as representative of doubly diffusive convection in which the more slowly diffusing component of the fluid is destabilizing. The model to be considered is that of a horizontal layer of fluid containing a destabilizing salinity gradient and a stabilizing temperature gradient large enough so that the density of the fluid decreases upwards. The layer is confined between two stress-free boundaries through which both heat and salt are perfectly conducted. These boundary conditions are not really representative of laboratory experiments in which hot salt water is placed over cold fresh water, and salt fingering occurs at the interface (Turner 1967; Stern & Turner 1969; Shirtcliffe & Turner 1970). The problem presented is, however, one which brings out the salient points of doubly diffusive convection, and it is felt that the major results obtained here have more general applicability. In addition, the fact that the problem for a free, perfectly conducting boundary is self-adjoint allows considerable progress to be made in the mathematical analysis.

The problem of wavelength selection in cellular convective problems is central to the present investigation. Much research has been carried out in this area since Malkus (1954), motivated by his experimental findings for thermal

convection, suggested that, among the manifold of solutions to the Boussinesq equations, the solution that maximizes the heat transport at a given value of the thermal Rayleigh number will be realized. Although this heuristic criterion seems to have approximate validity in many physical situations, it cannot be established mathematically. It is the stability of a particular flow that determines whether or not it will be seen in nature. This problem was formally solved for small amplitude convection by Schlüter, Lortz & Busse (1965). They showed that, in the case of a Boussinesq fluid, two-dimensional rolls constitute the only horizontal planform stable to infinitesimal perturbations at a temperature gradient slightly greater than its critical value. The wave band of stable rolls was shown to deviate only slightly from the value predicted at marginal stability. Busse (1967) studied numerically the stability of finite amplitude roll solutions of the Boussinesq equations for thermal convection between rigid perfectly conducting parallel plates. It was found that not all wavelengths of convective motion are stable, for nonlinear effects cause all but a small wave band of modes to be unstable. It is important to note that this result is in conflict with the concept of a single physically distinguished wavelength since Busse's analysis predicts a finite range of stable rolls. Malkus' idea, however, is compatible with Busse's analysis in that the flow which transports the most heat at a given thermal Rayleigh number has a wavelength that is found to fall within the region of stable rolls.

In contrast to the situation in thermal convection, in which the region of stable wavelengths always includes that at marginal stability, wavelengths in the salt finger instability are always observed to be much smaller than that at marginal stability. A major portion of this paper will be concerned with the dependence of various properties of the motion on its horizontal wavelength. For values of the relevant parameters near marginal stability, an expansion procedure that was used as a preliminary analysis is outlined. It is found that, in this parameter regime, the instability is quite similar to singly diffusive convection. For values of the relevant parameters well above marginal stability, the Galerkin method is used in a treatment similar to that of Busse (1967). Properties of the steady-state salt finger process are calculated and the stability of the finite amplitude flows thus found is examined. The small horizontal scale is found to be predictable as a consequence of the stability of the finite amplitude steady motion, and a 'preferred wavelength' is determined as that wavelength which is most stable to infinitesimal perturbations.

The effectiveness of salt fingers in transporting salt is described by the dependence of the salt Nusselt number on the salinity and temperature gradients. The salt Nusselt number is defined as the ratio of the actual rate of transport of salt to that which would occur if only diffusion were operative (the definition of Nusselt number for salt transport here is analogous to that of the usual Nusselt number for heat transport). The numerical results can be extrapolated to yield power laws describing this dependence. Since the power laws are closely approached by the numerical results, they should be representative over a wide range of Rayleigh numbers, even if the asymptotic state has not been reached in the range of parameters treated here. The salt flux is found to obey a power law qualitatively compatible with that observed in the laboratory experiments of Turner (1967).

2. Mathematical method

Consider a layer of fluid between parallel stress-free boundaries at $z = \pm \frac{1}{2}d$ which are perfectly conducting for both heat and solute. On the boundaries the solute concentration (salinity) and temperature are specified:

$$\begin{aligned} &\text{solute concentration:} \quad S(\tfrac{1}{2}d) = S_0 + \Delta S, \quad S(-\tfrac{1}{2}d) = S_0, \\ &\text{temperature:} \qquad\quad T(\tfrac{1}{2}d) = T_0 + \Delta T, \quad T(-\tfrac{1}{2}d) = T_0. \end{aligned}$$

The basic motionless state

$$T = T_0 + \Delta T(\tfrac{1}{2} + z/d), \quad S = S_0 + \Delta S(\tfrac{1}{2} + z/d)$$

is perturbed with disturbances in temperature, salinity, velocity and pressure: θ, Σ, $\mathbf{v}$ and p. In the Boussinesq approximation the governing equations for the perturbations are

$$\frac{\partial \mathbf{v}}{\partial t} + \mathbf{v}.\nabla\mathbf{v} = -\frac{1}{\rho_0}\nabla p + g\mathbf{k}(\alpha\theta - \beta\Sigma) + \nu\nabla^2\mathbf{v}, \tag{1}$$

$$\frac{\partial \theta}{\partial t} + \mathbf{v}.\nabla\theta = \kappa_T\nabla^2\theta - w\frac{\Delta T}{d}, \tag{2}$$

$$\frac{\partial \Sigma}{\partial t} + \mathbf{v}.\nabla\Sigma = \kappa_S\nabla^2\Sigma - w\frac{\Delta S}{d}, \tag{3}$$

$$\nabla.\mathbf{v} = 0, \tag{4}$$

where g = acceleration of gravity, α is the coefficient of thermal expansion, β is the density change due to a unit change in salinity, ΔT and ΔS are the temperature and salinity differences across a layer of depth d, ν is the kinematic viscosity, κ_T is the thermal diffusivity, κ_s is the salt diffusivity, $\mathbf{k}$ is the unit vector in the vertical direction, $\mathbf{v} = u\mathbf{x} + v\mathbf{y} + w\mathbf{k}$ and ρ_0 is the mean density. The boundary conditions are

$$\theta = \Sigma = w = \partial_{zz}w = 0 \quad \text{at} \quad z = \pm\tfrac{1}{2}d. \tag{5}$$

In order to carry out the analysis it is convenient to non-dimensionalize the equations as follows (an asterisk denotes a non-dimensional quantity):

$$\begin{aligned} &\mathbf{v} = (\kappa_s/d)\mathbf{v}^*, \quad t = (d^2/\kappa_s)t^*, \quad \theta = \tau\Delta T\theta^*, \\ &\Sigma = \Delta S\Sigma^*, \quad \mathbf{x} = d\mathbf{x}^*, \quad p = (\rho_0\kappa_s^2/d^2)p^*. \end{aligned}$$

Dropping the asterisks, the non-dimensional equations are

$$1/\Gamma[\partial\mathbf{v}/\partial t + \mathbf{v}.\nabla\mathbf{v}] = -\nabla p + (Ra\theta - R\Sigma)\mathbf{k} + \nabla^2\mathbf{v}, \tag{6}$$

$$\tau[\partial\theta/\partial t + \mathbf{v}.\nabla\theta] = -w + \nabla^2\theta, \tag{7}$$

$$\partial\Sigma/\partial t + \mathbf{v}.\nabla\Sigma = -w + \nabla^2\Sigma, \tag{8}$$

$$\nabla.\mathbf{v} = 0. \tag{9}$$

The following non-dimensional parameters have been introduced:

$$Ra = g\alpha\Delta T d^3/\nu\kappa_T, \quad Rs = g\beta\Delta S d^3/\nu\kappa_T, \quad \tau = \kappa_s/\kappa_T, \quad R = Rs/\tau, \quad \Gamma = \nu/\kappa_s.$$

We shall now make an approximation, consistent with the doubly diffusive property of the instability, which will considerably simplify the analysis. We are

interested in the limit characterized by the inequalities $\nu \gg \kappa_T \gg \kappa_s$, but with R and Ra finite. The inequalities $\kappa_T \gg \kappa_s$ and $\nu \gg \kappa_s$ are especially appropriate for salt water, for which $\kappa_T/\kappa_s \sim 10^2$ and $\nu/\kappa_s \sim 10^3$. Thus, in this 'small τ limit' the momentum and heat equations are linearized, and the only nonlinear equation remaining is that for the solute:

$$O = -\nabla p + (Ra\theta - R\Sigma)\mathbf{k} + \nabla^2 \mathbf{v}, \tag{10}$$

$$w = \nabla^2 \theta, \tag{11}$$

$$\partial\Sigma/\partial t + \mathbf{v}.\nabla\Sigma = -w + \nabla^2\Sigma, \tag{12}$$

$$\nabla.\mathbf{v} = 0. \tag{13}$$

The linear stability analysis of the salt finger instability was given by Stern (1960) and will not be reproduced here. It is sufficient to indicate that the instability sets in as a monotonically growing disturbance (exchange of stabilities) when R exceeds its critical value $R_c = Ra + \frac{27}{4}\pi^4$. Further applications of linear theory to the salt finger problem were carried out following the analysis of Stern. Walin (1964) treated the problem for an infinite fluid and found that convection against a stable density gradient will generally occur on a scale limited by internal parameters and not by the dimensions of the vessel. He noted that, as is evident from the condition for marginal stability, since $\tau \ll 1$ instability will occur unless the density is very stably stratified, i.e. for large R and Ra, instability is hindered only if $\alpha\Delta T > \beta\Delta S/\tau$. Nield (1967) treated the problem for general boundary conditions. Baines & Gill (1969) presented an exhaustive linear analysis for both this problem and the inverse problem: that of thermal convection in the presence of a stabilizing salinity gradient. They found, as did Stern, that when $Ra \gg Rs$ the infinitesimal mode with the largest rate of growth has a wavenumber $\alpha \sim Ra^{\frac{1}{4}}$. Yih (1970) has proved that, for values of the parameters of geophysical interest, the principle of exchange of stabilities holds.

For $R > R_c$ a convective motion is established in which those modes which grow most rapidly dominate initially. As the flow amplitude increases, interactions between the various modes occur, and nonlinear terms in the governing equations become important in allowing a steady-state flow to develop. In order to treat the problem for values of R and Ra just above those for marginal stability, an expansion in the small amplitude of the motion may be used. Since the analysis is very similar to that of Schlüter, Lortz & Busse (1965) it will not be reproduced here in detail. Such a treatment yields several results of interest. For values of R slightly in excess of $R_c = Ra + \frac{27}{4}\pi^4$, two-dimensional rolls transport more salt than any other horizontal planform and constitute the only type of motion stable to infinitesimal perturbations. (That the solute flux is the important quantity to look at is reasonable since it is the solute concentration this is destabilizing and thus drives the motion; since $\kappa_T \gg \kappa_s$, the temperature perturbation θ is small and the heat flux is only slightly modified by the convective motion.) This analysis also yields the following results for R near R_c.

(i) When R is expanded as $R = R_0 + \epsilon R_1 + \epsilon^2 R_2 + \ldots$, where ϵ is the small but finite amplitude of the motion, the results $R_0 = Ra + (\alpha^2 + \pi^2)^3/\alpha^2$ and $R_1 = 0$

follow. Here α is the horizontal wavenumber of the flow. For two-dimensional roll solutions, $R_2 = R_0/4(\alpha^2+\pi^2)$. Thus, to this order for two-dimensional flow,

$$\epsilon = \left(\frac{R-R_0}{R_2}\right)^{\frac{1}{2}} = 2\left[\frac{R-R_0}{R_0}(\alpha^2+\pi^2)\right]^{\frac{1}{2}}.$$

(ii) No subcritical instability is to be expected, since $R = R_0+\epsilon^2 R_2$ with $R_2 > 0$, $\epsilon^2 > 0$; thus, to this order, instability cannot set in at a lower value of R than R_0. This result can be proved more generally using the energy method.

(iii) The solute and thermal Nusselt numbers are related by

$$(Nu^s-1)/(Nu^t-1) = 1/\tau^2.$$

Since these findings indicate that two-dimensional motion is to be expected for small amplitude doubly diffusive convection, motion having the form of two-dimensional rolls will be considered here. Although this is an assumption made mainly for computational reasons, it is reasonable that two-dimensional motion may extend throughout the range of low to moderate values of R and Ra included in the present work. Three-dimensional motion in the form of fingers is realized in laboratory experiments at values of R and Ra considerably larger than those treated here; at these large values of R and Ra, the laboratory experiments are certainly in a turbulent rather than a laminar regime, and the three-dimensionality may be due to effects other than those included here. In any case, it is felt that the values of the salt transport calculated here are not grossly in error because of the two-dimensional model, and the flow of small horizontal scale predicted by the present analysis is, in fact, physically realized.

In order to treat the steady-state salt fingering process, we shall expand the variables in (10)–(13) in a double Fourier series (in x and z), keeping enough terms to ensure an accurate representation of the flow. The resulting system of coupled nonlinear ordinary differential equations, with time as the independent variable, may be integrated numerically to find the Fourier coefficients in the steady state. The solute flux can thus be calculated as a function of α^2 for given values of R and Ra. This method is particularly useful because it can be combined with a stability analysis (Busse 1967). The solution to the steady-state problem may be perturbed with infinitesimal disturbances whose growth rates may be determined as eigenvalues. Any disturbance with a growing time dependence indicates that the steady flow is unstable; otherwise it is stable.

In order to develop the equations to be solved, we shall introduce new notation. Since the vertical component of vorticity satisfies $\nabla^2(\partial v/\partial x - \partial u/\partial y) = 0$, the boundary conditions allow only the solution $\partial v/\partial x - \partial u/\partial y = 0$, if the possibility of rigid rotation is excluded. Since continuity, $\nabla.\mathbf{v} = 0$, must also be satisfied, we may write

$$v_i = \delta_i \phi, \quad \text{where} \quad \delta_i = (\partial_x\partial_z, \partial_y\partial_z, -\nabla_1^2) \tag{14}$$

and

$$\nabla_1^2 = (\partial_{xx}+\partial_{yy}).$$

In two dimensions, x and z, the equations become

$$\nabla^4\phi = \theta Ra - \Sigma R, \quad \partial_{xx}\phi = -\nabla^2\theta, \tag{15, 16}$$

$$\partial_t \Sigma = -\delta_j\phi\,\partial_j\Sigma + \partial_{xx}\phi + \nabla^2\Sigma, \tag{17}$$

where now

$$\nabla^2 = (\partial_{xx} + \partial_{zz}) \quad \text{and} \quad \delta_i = (\partial_x \partial_z, -\partial_{xx}).$$

We may eliminate θ between (15) and (16) to obtain

$$(\nabla^6 + Ra\,\partial_{xx})\phi = -R\nabla^2\Sigma. \tag{18}$$

Equations (17) and (18) are those to be studied.

3. The finite amplitude steady solutions

Assuming that Σ and ϕ are periodic in the horizontal, expand Σ in a Fourier series that satisfies free perfectly conducting boundary conditions at $z = \pm\frac{1}{2}$:

$$\Sigma = \sum_{\lambda,\nu} a_{\lambda\nu}(t)\, e^{i\lambda\alpha x} \sin \nu\pi(z+\tfrac{1}{2}), \tag{19}$$

where $-\infty < \lambda < \infty, 1 \leqslant \nu < \infty$ and $a_{\lambda\nu} = a^*_{-\lambda\nu}$, where $*$ denotes the complex conjugate. Similarly, expand ϕ as

$$\phi = \sum_{\lambda,\nu} b_{\lambda\nu}(t)\, e^{i\lambda\alpha x} \phi_\nu(z), \tag{20}$$

where the same summation limits apply as for Σ, and $b_{\lambda\nu} = b^*_{-\lambda\nu}$. We may solve for $b_{\lambda\nu}(t)\phi_\nu(z)$ using the linear equation (18). The particular solution is

$$b_{\lambda\nu}(t)\phi_\nu(z) = -\frac{R[(\nu\pi)^2 + (\lambda\alpha)^2]\sin\nu\pi(z+\frac{1}{2})}{\{[(\nu\pi)^2 + (\lambda\alpha)^2]^3 + (\lambda\alpha)^2 Ra\}}\, a_{\lambda\nu}(t). \tag{21}$$

Since the particular solution satisfies the boundary conditions, the homogeneous problem has a vanishing solution. Thus we may substitute the Fourier series for Σ and ϕ into the remaining nonlinear equation (17), multiply by

$$e^{-i\rho\alpha x} \sin \eta\pi(z+\tfrac{1}{2}),$$

and integrate over the layer to obtain the following set of coupled first-order ordinary differential equations for the $a_{\lambda\nu}(t)$:

$$\begin{aligned}
\dot{a}_{\lambda\nu} = {} & \left(\frac{R[(\lambda\alpha)^2 + (\nu\pi)^2](\lambda\alpha)^2}{[(\lambda\alpha)^2 + (\nu\pi)^2]^3 + (\lambda\alpha)^2 Ra} - [(\lambda\alpha)^2 + (\nu\pi)^2]\right) a_{\lambda\nu} \\
& - \frac{R\alpha^2\pi}{2} \sum_{\rho=-\infty}^{\infty} \left(\sum_{\eta=1}^{\nu-1} \frac{[(\rho\alpha)^2 + (\eta\pi)^2](\rho\eta\lambda - \rho^2\nu)}{[(\rho\alpha)^2 + (\eta\pi)^2]^3 + (\rho\alpha)^2 Ra}\, a_{\rho\eta} a_{|\lambda-\rho|,\nu-\eta} \right. \\
& - \sum_{\eta=\nu+1}^{\infty} \frac{[(\rho\alpha)^2 + (\eta\pi)^2](\rho\eta\lambda - \rho^2\nu)}{[(\rho\alpha)^2 + (\eta\pi)^2]^3 + (\rho\alpha)^2 Ra}\, a_{\rho\eta} a_{|\lambda-\rho|,\eta-\nu} \\
& \left. + \sum_{\eta=1}^{\infty} \frac{[(\rho\alpha)^2 + (\eta\pi)^2](\rho\eta\lambda + \rho^2\nu)}{[(\rho\alpha)^2 + (\eta\pi)^2]^3 + (\rho\alpha)^2 Ra}\, a_{\rho\eta} a_{|\lambda-\rho|,\eta+\nu} \right).
\end{aligned} \tag{22}$$

As Busse (1967) has pointed out, the symmetry of the equations allows the analysis to be simplified. The equations contain a closed subset in which only coefficients with even $|\lambda| + \nu$ appear. The set with odd $|\lambda| + \nu$ leads to decaying solutions only, and so only the set with even $|\lambda| + \nu$ need be treated in the following numerical work. It is also appropriate to examine a finite subset of the equations

for which $|\lambda| + \nu \leqslant N$, where N is a positive even integer. This is a commonly used method and is explained in some detail by Veronis (1966).

In this way systems of equations with $N = 4, 6, 8, 10, 12, 14$ and 16 were integrated numerically, for a range of values of R for fixed values of Ra, using a modified predictor-corrector method due to Hammings (Ralston & Wilf 1960) and a rational extrapolation method due to Bulirsch & Stoer (1966). Small initial values for the coefficients were used, although the asymptotic steady-state solution appeared to be unique, since it was reached independently of the choice of initial conditions. In order to speed convergence, in many cases results from calculations with lower values of N were used as initial values. The time step was varied between 0·01 and 0·0005 to ensure accuracy, and integration was carried out until a steady state was reached. The criterion for convergence was taken to be

$$\left|\frac{da_{\lambda\nu}(t)}{dt}\right| < 10^{-4}|a_{\lambda\nu}|$$

and was usually attained before the integration reached $t = 1$; since the time was non-dimensionalized with respect to the solute diffusion time, the longest time scale in the problem, this is reasonable. The validity of the results was verified by examining the value of the solute Nusselt number

$$Nu^s = 1 + \pi \sum_{\nu} \nu a_{0\nu}$$

as a function of N: if Nu^s varied by less than 1 % as N was increased from N to $N+2$, the representation with $|\lambda| + \nu \leqslant N$ was considered sufficiently accurate. Since Nu^s is a rapidly convergent function of N when N is large enough, the results for Nu^s are considered to have an error no larger than 1 %.

As expected, for a given Ra, larger values of N are necessary as R increases. Also, for fixed R/Ra more terms are required in the representations as Ra increases because, for high values of Ra, higher modes become important at a lower ratio R/Ra than for lower Ra; for this reason, for large Ra, the numerical solutions may be obtained only up to a value of R/Ra that is lower than that possible for smaller Ra. In addition, as Ra is increased for fixed R, fewer terms are needed in the representation because the ratio R/Ra is thereby decreased; for this reason, higher values of R may be examined as Ra is increased.

Using the method just described, the Fourier coefficients, and thus the flow fields, were calculated for given values of R and Ra as α^2 was varied. Of primary interest was the maximum value of Nu^s and the value of α^2 at which the maximum occurred. Seven values of Ra were used: $0, 10^3, 5\times10^3, 10^4, 4\times10^4, 10^5$ and 2×10^5. The value $Ra = 0$ corresponds to singly diffusive convection driven by an unstable salinity gradient and was investigated as a check on the numerical method and for a comparison between singly and doubly diffusive convection. For $N = 2$ an analytic expression for Nu^s can be derived:

$$\begin{aligned} Nu^s &= 1 + 2\pi a_{02} \\ &= 3 - \frac{2}{R}\left[Ra + \frac{(\alpha^2+\pi^2)^3}{\alpha^2}\right], \end{aligned} \tag{23}$$

α^2	$Nu^s(N = 2)$	$Nu^s(N = 6)$	$Nu^s(N = 8)$
$\frac{1}{8}\pi^2$	2·389	2·818	2·821
$\frac{1}{4}\pi^2$	2·424	2·971	2·976
$\frac{1}{2}\pi^2$	2·432	3·095	3·112
$\frac{3}{4}\pi^2$	2·430	3·157	3·174
π^2	2·422	3·195	3·219
$\frac{3}{2}\pi^2$	2·400	3·277	3·294
$2\pi^2$	2·369	3·332	3·359
$\frac{5}{2}\pi^2$	2·330	3·388	3·411
$3\pi^2$	2·292	3·371	3·392
$\frac{7}{2}\pi^2$	2·253	3·337	3·345
$4\pi^2$	2·196	3·260	3·267
$5\pi^2$	2·079	3·023	3·031

TABLE 1. Nu^s for $Ra = 5000$ and $R = 20000$ as a function of α^2 and N

so that, to this order, Nu^s approaches the value 3 as $R \to \infty$ for a fixed value of Ra. This expression certainly underestimates Nu^s for values of R/R_c greater than about 2, but is accurate for R near its critical value. Also, it predicts that Nu^s reaches its maximum at a given R and Ra when $\alpha^2 = \frac{1}{2}\pi^2$, which is the same wavenumber (squared) as at marginal stability. This result is not borne out when larger N is used for larger values of R/R_c, where it is found that larger values of α^2 are required to maximize Nu^s. In table 1 the value of Nu^s is shown, as calculated from the systems of equations with N as indicated, for $Ra = 5000$ and $R = 20000$. In this case, the $N = 6$ and $N = 8$ values for Nu^s always differ by less than 1 %, so the values are acceptable. The value of α^2 that maximizes Nu^s corresponds to a shorter wavelength than that at marginal stability.

In table 2 are given the values of the maximum Nu^s as a function of R and Ra and the value of α^2 at which the maxima occur; also shown is the value of N necessary to achieve accurate results. It is evident from the values of Nu^s in this table that Nu^s is a function of neither $R - R_c$ nor R/R_c alone, but depends on some combination of R and Ra. The total convective flux RNu^s does seem to depend on $R - R_c$ and is discussed below.

Figures 1 (*a*) and (*b*) show the dependence of Nu^s on R and α^2 for two cases: $Ra = 0$ and $Ra = 10^4$. These allow a clear comparison to be made between the singly and doubly diffusive cases. Several important results are to be seen in table 2 and these two figures. The wavenumber for which Nu^s is maximized increases considerably in the doubly diffusive cases ($Ra \neq 0$) as R increases away from R_c, but the singly diffusive case ($Ra = 0$) shows only a very slight increase of the maximizing wavenumber, a result reported in many theoretical investigations. The doubly diffusive cases also show the tendency for the maximizing wavenumber to be an increasing function of Ra, for constant values of R/R_c. In the next section we shall examine the stability of the finite amplitude roll solutions found here. Since the preference of the flow for a particular wavenumber lies in the stability of that wavenumber to perturbations, the correspondence between maximum salt transport and stability will be seen there.

In figure 2 the convective solute flux $R(Nu^s - 1)$ is plotted as a function of

Ra	R	$Nu^s_{\max}$	α^2/π^2 at $Nu^s_{\max}$	N
0	1000	1·74	0·52	4
	3000	3·21	0·57	6
	5000	3·88	0·63	6
	10000	4·92	0·73	8
	15000	5·58	0·80	10
	20000	6·19	0·86	12
	30000	7·13	0·90	14
	40000	7·86	0·93	16
1000	3000	2·01	0·60	6
	5000	2·74	0·71	6
	10000	3·74	1·05	8
	15000	4·36	1·39	8
	20000	4·85	1·60	10
	30000	5·62	1·85	12
5000	10000	2·04	0·93	6
	20000	3·41	2·60	8
	40000	5·00	4·02	10
	60000	6·01	5·11	12
10000	15000	1·62	1·01	6
	20000	2·33	2·13	8
	30000	3·41	2·90	10
	40000	4·17	4·28	10
	60000	5·32	5·00	12
	80000	6·24	5·67	14
40000	50000	1·59	1·97	6
	60000	2·20	2·63	8
	80000	3·42	3·51	10
	120000	5·09	5·28	12
	160000	6·34	5·60	14
100000	150000	2·64	6·04	10
	200000	4·32	7·96	12
	300000	6·73	10·88	16
200000	300000	3·14	8·89	12
	400000	5·28	10·20	14

TABLE 2

$(R - R_c)$ for constant values of Ra. The convective flux in the singly diffusive case is closely approximated by the power law $R(Nu^s - 1) = 0{\cdot}135(R - R_c)^{1{\cdot}37}$ for $R > 15000$, in excellent agreement with Veronis' (1966) similar treatment of this problem (his calculations were for Pr = 6·8, whereas the present results are for Pr$\to\infty$). The total transport in this case, RNu^s, seems to approach a power law $RNu^s \sim 0{\cdot}29(R - R_c)^{1{\cdot}33}$, but the highest value of R used (40000) and its corresponding Nusselt number (7·86) may not be large enough to allow an accurate power law for the total flux to be calculated. Thus the power law for the convective flux $R(Nu^s - 1)$ is a more reliable result than that for RNu^s.

For $Ra \neq 0$ the doubly diffusive character of the instability manifests itself. Owing to the small τ limit being used, the values of Rs and τ may not be specified separately, but only their ratio R used. On the one hand, this is a disadvantage of

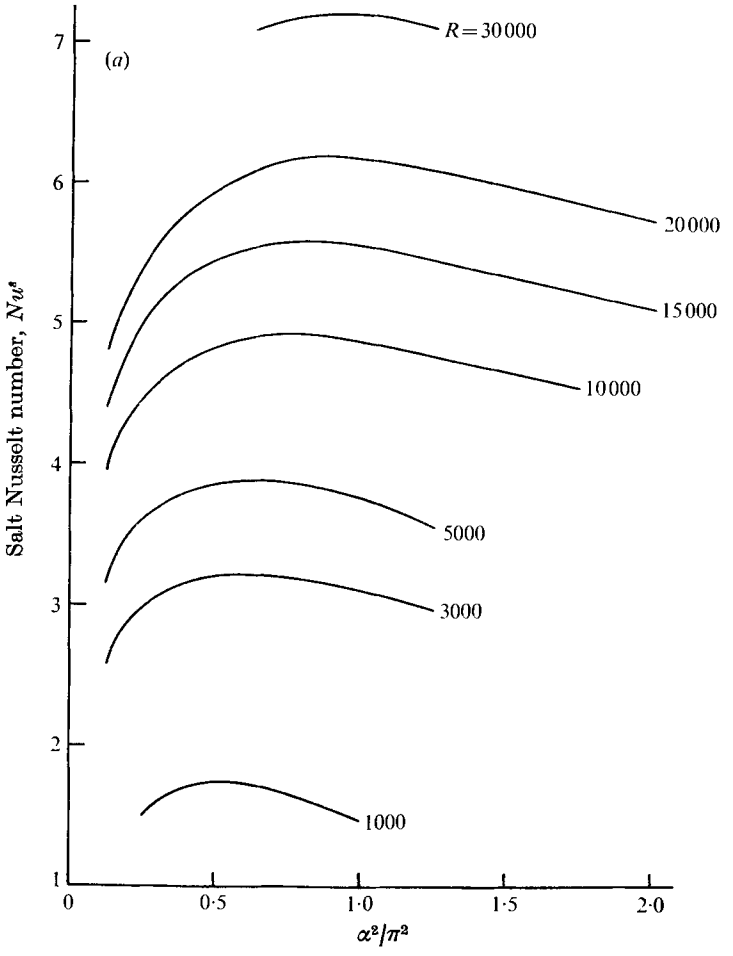

FIGURE 1(*a*). For legend see p. 364.

the limit, since the effects of varying Rs and τ separately could not be treated. However, since this limit is valid for problems of oceanographic interest, it indicates that the ratio is the important quantity, and not the values of Rs and τ individually, as shown by (18). Before the small τ limit was recognized as useful, a system of equations that was valid for any τ was developed. Several calculations were carried out with Ra, Rs and τ as independent parameters. As τ was decreased to values less than $\sim 0{\cdot}1$, it was found that the two systems of equations led to essentially identical results for both the heat and salt flux. As an example, for $Ra = 5 \times 10^3$, $Rs = 4 \times 10^3$, $\tau = 0{\cdot}1$ ($R = 4 \times 10^4$), $\alpha^2 = \frac{1}{2}\pi^2$ and $N = 10$, the more general system gave $Nu^s = 4{\cdot}2014$ and $Nu^t = 1{\cdot}2008$, whereas the small τ system gave $Nu^s = 4{\cdot}1834$ and $Nu^t = 1{\cdot}2081$. These results differ by considerably less than the 1 % error considered to be inherent in the computations for the Nusselt numbers. Therefore, the small τ equations are felt to be quite accurate for values of the parameters of geophysical interest.

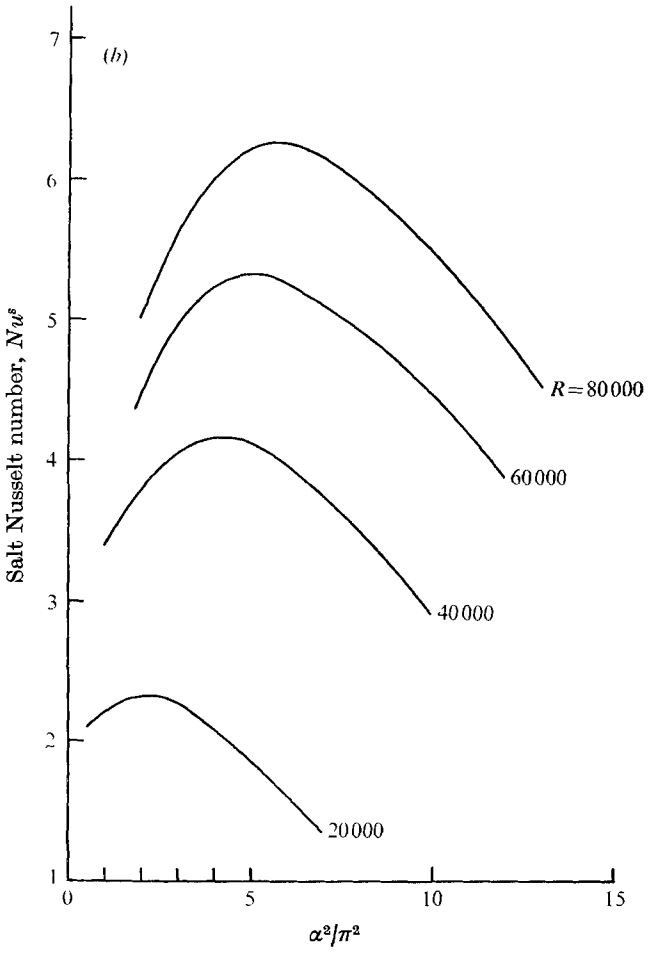

FIGURE 1. Nu^s *vs.* R and α^2. (*a*) $Ra = 0$; the wavenumber at which Nu^s is maximized, at a given value of R, is only weakly dependent on R. (*b*) $Ra = 10^4$; the wavenumber at which Nu^s is maximized, at a given value of R, increases rapidly with R.

As can be seen in figure 2, for $Ra \neq 0$ different power laws were obtained for different values of Ra. As Ra increases, the lines appear to merge into a single one. However, the possibility that there is an additional weak inverse dependence of $R(Nu^s - 1)$ on Ra cannot be ruled out as a result of the present investigation. Further analysis, perhaps an analytical approximation, is needed to determine this dependence. For $Ra \geqslant 10^4$, the convective flux may be approximated by $R(Nu^s - 1) = 0{\cdot}11\ (R - R_c)^{1{\cdot}36}$. This result is very similar to that obtained in the case $Ra = 0$. The slightly lower exponent is probably not of significance and is felt to be due to the fact that an asymptotic limit has not been approached as closely as in the calculations for $Ra = 0$. In the $Ra = 0$ case, the largest value of R (4×10^4) represents 60·88 times the critical value of R. For the doubly diffusive cases which are included in this power law, the largest value attained by R/R_c is 7·51. (This occurs when $R = 8 \times 10^4$, $Ra = 10^4$.)

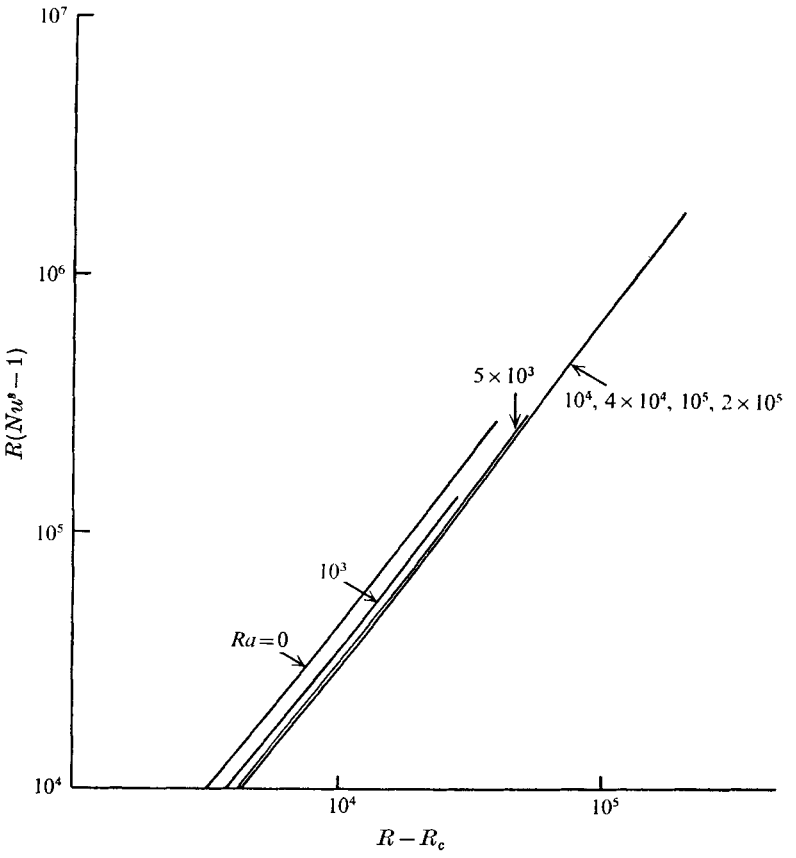

FIGURE 2. Convective solute flux $R(Nu^s-1)$ *vs.* $(R-R_c)$ for (*a*) $Ra = 0$, (*b*) $Ra = 10^3$, (*c*) $Ra = 5\times10^3$, (*d*) $Ra = 10^4, 4\times10^4, 10^5, 2\times10^5$.

The reason for the fact that a lower value of R/R_c is attainable as Ra increases was pointed out earlier. It is expected that for large R/R_c the power law for the total salt flux is given by $RNu^s = \text{constant}\times(R-Ra)^{\frac{4}{3}}$.

Figures 3(*a*) and (*b*) show lines of constant salinity (isohalines) for a half-cell for two cases of interest: $R = 4\times10^4$, $Ra = 5\times10^3$, $\alpha^2 = 4\pi^2$ and $R = 1{\cdot}5\times10^5$, $Ra = 10^5$, $\alpha^2 = 6\pi^2$. Both of these are for values of α^2 very near that which maximizes Nu^s at these values of R and Ra. It is evident from these figures that the amplitude of the motion is not a function of $R-R_c$ alone, but depends also on R/R_c. The isohalines, which in the absence of convective motion are parallel and equally spaced, are much more affected by the motion in the first case than in the second, even though $R-R_c$ is larger in the latter. Since we are dealing with the small τ limit, the isotherms are only slightly affected by the motion and remain almost parallel, as in the static configuration; for this reason no isotherms are shown here.

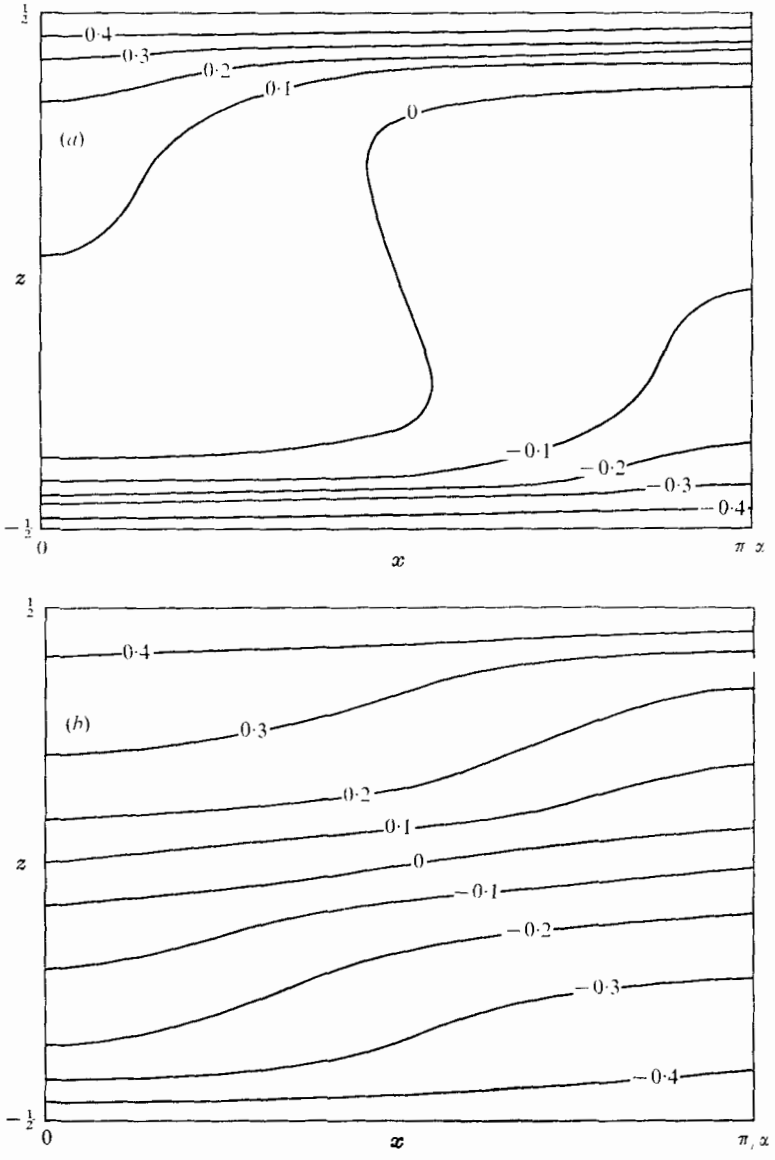

FIGURE 3. Isohalines for two doubly diffusive cases. (*a*) $Ra = 5\times10^3$, $R = 4\times10^4$, $\alpha^2 = 4\pi^2$. (*b*) $Ra = 10^5$, $R = 1{\cdot}5\times10^5$, $\alpha^2 = 6\pi^2$. The regions shown are a half-cell: $-\frac{1}{2} \leqslant z \leqslant \frac{1}{2}$, $0 \leqslant x \leqslant \pi/\alpha$. Both fields are from calculations with $N = 10$.

4. Stability of the steady finite amplitude solutions

In order to determine the stability of the steady flows determined in the previous section, we superpose three-dimensional disturbances $\tilde{\phi}, \tilde{\Sigma}$ and $\tilde{\theta}$ on the steady-state solutions. The equations governing the perturbations are

$$(\nabla^6 + Ra\nabla_1^2)\tilde{\phi} = -R\nabla^2\tilde{\Sigma}, \tag{24}$$

$$\partial\tilde{\Sigma}/\partial t = -\delta_j\tilde{\phi}\,\partial_j\Sigma - \delta_j\phi\,\partial_j\tilde{\Sigma} + \nabla_1^2\tilde{\phi} + \nabla^2\tilde{\Sigma}. \tag{25}$$

Look at perturbations of the same spatial periodicity in x and z as the steady solutions and multiplied by a function periodic in x and y and satisfying free perfectly conducting boundary conditions at $z = \pm\frac{1}{2}$:

$$\tilde{\Sigma} = \sum_{\lambda,\nu} \tilde{a}_{\lambda\nu} e^{i\lambda\alpha x} \sin \nu\pi(z+\tfrac{1}{2})\, e^{i(dx+by)}\, e^{pt},$$

$$\tilde{\phi} = \sum_{\lambda,\nu} \tilde{b}_{\lambda\nu} e^{i\lambda\alpha x} \tilde{\phi}_\nu(z)\, e^{i(dx+by)}\, e^{pt}.$$

Thus, from (24), we find the particular solution:

$$\tilde{\phi} = -e^{pt} \sum_{\lambda,\nu} \frac{R[(\lambda\alpha+d)^2+b^2+(\nu\pi)^2]\tilde{a}_{\lambda\nu} e^{i\lambda\alpha x} \sin \nu\pi(z+\frac{1}{2})\, e^{i(dx+by)}}{[(\lambda\alpha+d)^2+b^2+(\nu\pi)^2]+{}^3Ra[(\lambda\alpha+d)^2+b^2]}. \tag{26}$$

In the same manner as that used for the steady problem, a set of equations is developed that may be solved for the eigenvalues p, using the same value of N that was used in the corresponding (same R, Ra and α^2) steady problem.

If we were interested in calculating all the eigenvalues p, this would be a formidable task, since the matrix involved can be as large as 72×72 (for $N = 16$). However, our main interest is to determine whether, given R, Ra and α^2, there is an eigenvalue with a positive real part. We know that, near R_c, there is a region of stable rolls, so that all eigenvalues have negative real parts in that region. The method, then, is to move outwards from $\alpha^2 = \frac{1}{2}\pi^2$, at a given value of R and Ra, both to larger and smaller values of α^2 and look for the first time an eigenvalue with a positive real part occurs. Thus an iterative procedure based on Sylvester's theorem was used to calculate the eigenvalue with the lowest absolute value (see, for example, Frazer, Duncan & Collar 1952). As a test of the method, all the eigenvalues were calculated for $N = 4$ when R was near R_c. The only positive eigenvalue was found to be real in all cases. Also, the iterative procedure used for larger N will not converge if the eigenvalue with the lowest absolute value is complex, and convergence was always attained. Thus the iterative method was used with confidence to determine the growth rate p, and unstable solutions, corresponding to positive p, were readily found.

When R is near its critical value R_c two types of disturbances must be considered. For $\alpha > \pi/\sqrt{2}$ disturbance rolls at right angles to the original rolls limit the region of stable rolls most strongly; a numerical analysis as outlined above will be used to treat this case. For $\alpha < \pi/\sqrt{2}$ and R less than some value dependent on Ra, the steady flow becomes unstable to disturbance rolls oriented at a small angle to the original roll. Although the same numerical procedure may be used to treat this type of perturbation, the growth rate is proportional to the square of the y component of the disturbance wave vector. For this reason it becomes difficult to determine the stability boundary accurately. The stability boundary for this particular disturbance can be obtained, however, by an analytical criterion similar to that described by Lortz (1968).

In the small τ, large Γ limit treated here, the equations for the steady rolls may be written as

$$\delta_j \phi\, \partial_j \left(\nabla^4 + Ra \frac{\nabla_1^2}{\nabla^2}\right) \phi = -R\nabla_1^2 \phi + (\nabla^6 + Ra\nabla_1^2)\, \phi, \tag{27}$$

where the operator ∇_1^2/∇^2 is well defined because we are interested in solutions for ϕ of the form

$$\phi = \sum_{\lambda,\nu} b_{\lambda\nu} e^{i\lambda\alpha x} \sin \nu\pi(z+\tfrac{1}{2}).$$

Similarly, the disturbance $\tilde{\phi}$ satisfies

$$\frac{\partial}{\partial t}\left(\nabla^4 + Ra\frac{\nabla_1^2}{\nabla^2}\right)\tilde{\phi} + \delta_j\tilde{\phi}\,\partial_j\left(\nabla^4 + Ra\frac{\nabla_1^2}{\nabla^2}\right)\phi + \delta_j\phi\,\partial_j\left(\nabla^4 + Ra\frac{\nabla_1^2}{\nabla^2}\right)\tilde{\phi}$$
$$= -R\nabla_1^2\tilde{\phi} + (\nabla^6 + Ra\nabla_1^2)\tilde{\phi}. \tag{28}$$

We are interested in disturbances $\tilde{\phi}$ which are almost aligned with the original rolls. Thus, we write

$$\tilde{\phi} = f(x,z)e^{\sigma t}e^{imy},$$

where m is small, and expand

$$f = f_0 + m^2 f_1 + \ldots,$$
$$\sigma = \sigma_0 + m^2\sigma_1 + m^4\sigma_2 + \ldots.$$

Then f satisfies

$$\sigma\left[(\nabla^2 - m^2)^2 + Ra\frac{\partial_{xx} - m^2}{\nabla^2 - m^2}\right]f + \partial_{xz}f\,\partial_x\left(\nabla^4 + Ra\frac{\partial_{xx}}{\nabla^2 - m^2}\right)\phi$$
$$- (\partial_{xx} - m^2)f\,\partial_z\left(\nabla^4 + Ra\frac{\partial_{xx}}{\nabla^2 - m^2}\right)\phi + \partial_{xz}\phi\,\partial_x\left[(\nabla^2 - m^2)^2 + Ra\frac{\partial_{xx} - m^2}{\nabla^2 - m^2}\right]f$$
$$- \partial_{xx}\phi\,\partial_z\left[(\nabla^2 - m^2)^2 + Ra\frac{\partial_{xx} - m^2}{\nabla^2 - m^2}\right]f$$
$$= -R(\partial_{xx} - m^2)f + [(\nabla^2 - m^2)^3 + Ra(\partial_{xx} - m^2)]f. \tag{29}$$

The equation for f_0 is

$$\partial_{xz}f_0\,\partial_x\left[\nabla^4 + Ra\frac{\partial_{xx}}{\partial_{zz} + \partial_{xx}}\right]\phi - \partial_{xx}f_0\,\partial_z\left[\nabla^4 + Ra\frac{\partial_{xx}}{\partial_{zz} + \partial_{xx}}\right]\phi$$
$$+ \partial_{xz}\phi\,\partial_x\left[\nabla^4 + Ra\frac{\partial_{xx}}{\nabla^2}\right]f_0 - \partial_{xx}\phi\,\partial_z\left[\nabla^4 + Ra\frac{\partial_{xx}}{\nabla^2}\right]f_0$$
$$+ R\,\partial_{xx}f_0 - (\nabla^6 + Ra\,\partial_{xx})f_0 = 0. \tag{30}$$

A solution of this equation, with $\sigma_0 = 0$, is $f_0 = \partial_x\phi$, where ϕ is the steady roll solution. The $O(m^2)$ equation is

$$\partial_{xz}f_1\,\partial_x\left[\nabla^4 + Ra\frac{\partial_{xx}}{\nabla^2}\right]\phi - \partial_{xx}f_1\,\partial_z\left[\nabla^4 + Ra\frac{\partial_{xx}}{\nabla^2}\right]\phi + \partial_{xz}\phi\,\partial_x\left[\nabla^4 + Ra\frac{\partial_{xx}}{\nabla^2}\right]f_1$$
$$- \partial_{xx}\phi\,\partial_z\left[\nabla^4 + Ra\frac{\partial_{xx}}{\nabla^2}\right]f_1 + R\,\partial_{xx}f_1 - (\nabla^6 + Ra\,\partial_{xx})f_1$$
$$= -\sigma_1\left[\nabla^4 + Ra\frac{\partial_{xx}}{\nabla^2}\right]f_0 - f_0\,\partial_z\left[\nabla^4 + Ra\frac{\partial_{xx}}{\nabla^2}\right]\phi - Ra\,\partial_{xz}\phi\,\partial_x\left[\frac{\nabla_1^2}{\nabla^4} - \frac{1}{\nabla^2}\right]f_0$$
$$+ Ra\,\partial_{xx}\phi\,\partial_z\left(\frac{\nabla_1^2}{\nabla^4} - \frac{1}{\nabla^2}\right)f_0 + (R - Ra)f_0 - 3\nabla^4 f_0 + 2\,\partial_{xz}\phi\,\partial_x\nabla^2 f_0 - 2\partial_{xx}\phi\,\partial_z\nabla^2 f_0. \tag{31}$$

This equation is solvable if and only if

$$\sigma_1 \int_0^1 dz \int_0^{2\pi/\alpha} dx\, \psi \left(\nabla^4 + Ra \frac{\partial_{xx}}{\nabla^2}\right) f_0$$
$$= \int_0^1 dz \int_0^{2\pi/\alpha} dx\, \psi \left[-f_0 \partial_z \left(\nabla^4 + Ra \frac{\partial_{xx}}{\nabla^2}\right) \phi - Ra\, \partial_{xz}\phi\, \partial_x \left(\frac{\nabla_1^2}{\nabla^4} - \frac{1}{\nabla^2}\right) f_0 \right.$$
$$\left. + Ra\, \partial_{xx}\phi\, \partial_z \left(\frac{\nabla_1^2}{\nabla^4} - \frac{1}{\nabla^2}\right) f_0 \quad + (R - Ra) f_0 - 3\nabla^4 f_0 + 2\partial_{xz}\phi\, \partial_x \nabla^2 f_0 - 2\partial_{xx}\phi\, \partial_z \nabla^2 f_0 \right], \tag{32}$$

where ψ is the solution to the problem that is adjoint to (30) plus the free perfectly conducting boundary conditions

$$R\partial_{xx}\psi - (\nabla^6 + Ra\,\partial_{xx})\psi + \partial_{xz}\left[\psi \partial_x \left(\nabla^4 + Ra \frac{\partial_{xx}}{\nabla^2}\right)\phi\right] - \partial_{xx}\left[\psi \partial_z \left(\nabla^4 + Ra \frac{\partial_{xx}}{\nabla^2}\right)\phi\right]$$
$$- \partial_x \left(\nabla^4 + Ra \frac{\partial_{xx}}{\nabla^2}\right)(\psi \partial_{xz}\phi) + \partial_z \left[\left(\nabla^4 + Ra \frac{\partial_{xx}}{\nabla^2}\right)(\psi \partial_{xx}\phi)\right] = 0. \tag{33}$$

Once again, a solution may be easily found and is $\psi = \partial_x \phi$. The solvability condition becomes

$$\sigma_1 \int_0^1 dz \int_0^{2\pi/\alpha} dx \frac{\partial\phi}{\partial x} \left(\nabla^4 + Ra \frac{\partial_{xx}}{\nabla^2}\right) \frac{\partial\phi}{\partial x}$$
$$= \int_0^1 dz \int_0^{2\pi/\alpha} dx \frac{\partial\phi}{\partial x} \left[-\frac{\partial\phi}{\partial x} \frac{\partial}{\partial z} \left(\nabla^4 + Ra \frac{\partial_{xx}}{\nabla^2}\right)\phi - Ra \frac{\partial^2\phi}{\partial_x \partial_z} \frac{\partial}{\partial x} \left(\frac{\nabla_1^2}{\nabla^4} - \frac{1}{\nabla^2}\right) \frac{\partial\phi}{\partial x} \right.$$
$$+ Ra \frac{\partial^2\phi}{\partial x^2} \frac{\partial}{\partial z} \left(\frac{\nabla_1^2}{\nabla^4} - \frac{1}{\nabla^2}\right) \frac{\partial\phi}{\partial x} + (R - Ra) \frac{\partial\phi}{\partial x} + 2 \frac{\partial^2\phi}{\partial_x \partial_z} \frac{\partial}{\partial x} \nabla^2 \frac{\partial\phi}{\partial x}$$
$$\left. - 2 \frac{\partial^2\phi}{\partial x^2} \frac{\partial}{\partial z} \nabla^2 \frac{\partial\phi}{\partial x} - 3\nabla^4 \frac{\partial\phi}{\partial x} \right]. \tag{34}$$

In the limit $Ra \to 0$ this expression is identical to that obtained by Lortz, and corresponds to singly diffusive convection.

Relation (34) determines σ_1 if a solution for ϕ is known. The steady solutions found using the Fourier series representation for ϕ were used to determine the stability of the roll solutions to perturbations of the type treated here. This analysis yields the stability boundary for $\alpha < \pi/\sqrt{2}$ and for R less than some value which is a function of Ra. Above that value of R, this stability boundary intersects a boundary for disturbances at larger angles of inclination to the original roll, and is not of interest beyond that point.

For $\alpha > \pi/\sqrt{2}$, and for $\alpha < \pi/\sqrt{2}$ when R is greater than a certain value dependent on Ra, the range of stability of the steady solutions was found to be determined by the system of equations for which $N = |\lambda| + \nu$ is odd. Stability of the rolls to these perturbations was carried out using the iterative procedure outlined above. Since in all the computer runs it was found that the maximum growth rate of the disturbances always occurred for $d = 0$, further discussion of the dependence of p on d is omitted. It is useful to note that if only the lowest terms are included in the expansion, the roll solutions are unstable if

$$\frac{(b^2 + \pi^2)^3}{b^2} < \frac{(\alpha^2 + \pi^2)^3}{\alpha^2};$$

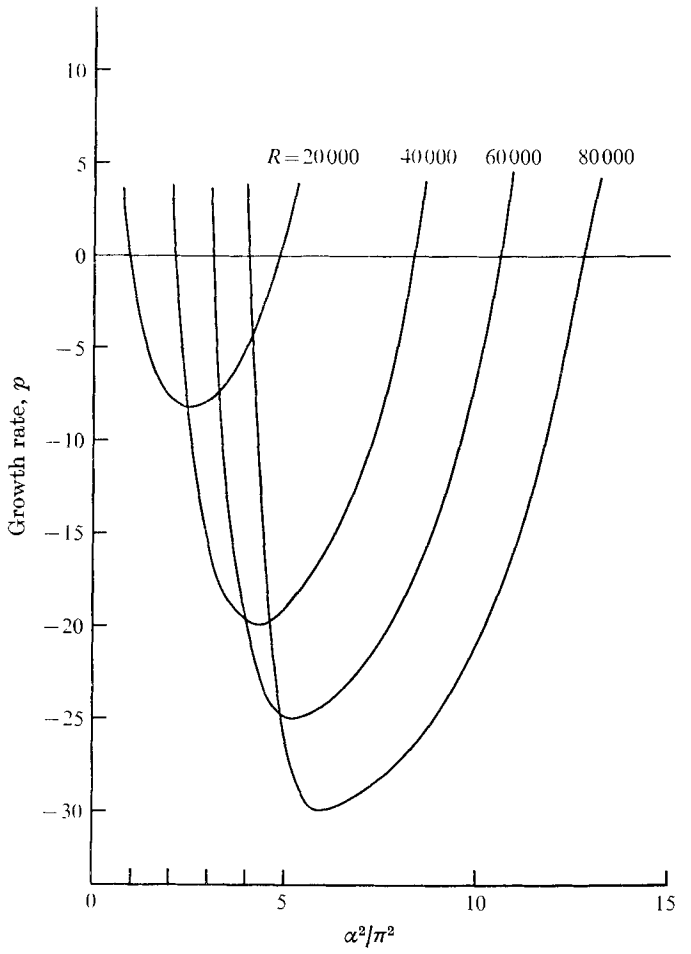

FIGURE 4. Disturbance growth rate p *vs.* R and α^2 for $Ra = 10^4$. The curves represent the largest growth rate p at a given (R, α^2) point.

that is, if $\alpha^2 \neq \frac{1}{2}\pi^2$ there is a perturbation b to which the original roll is unstable. This result is contained in the investigation of thermal convection by Busse (1971). Higher-order terms modify this result. Figure 4 shows the relevant growth rates of the disturbance as a function of α^2 for $Ra = 10^4$ for several values of R. The growth rate of the most critical disturbance shown here (corresponding to the value of b which maximizes p) varies continuously as the wavenumber α of the finite amplitude roll solution is varied. It is positive outside a limited band of wavenumbers and reaches a minimum at a wavenumber which we shall call the 'most stable' wavenumber. It is clear that, as R is increased for a given value of Ra, the most stable wavenumber increases in much the same way as does the wavenumber at which Nu^s is maximized. Consideration of all of the results of all the computations carried out for doubly diffusive cases indicates that the band of stable rolls shows a definite tendency for shorter wavelengths to be preferred as R/R_c is increased and as Ra is increased at a given value of R/R_c. Similar results for the singly diffusive problem, $Ra = 0$, show no such tendency.

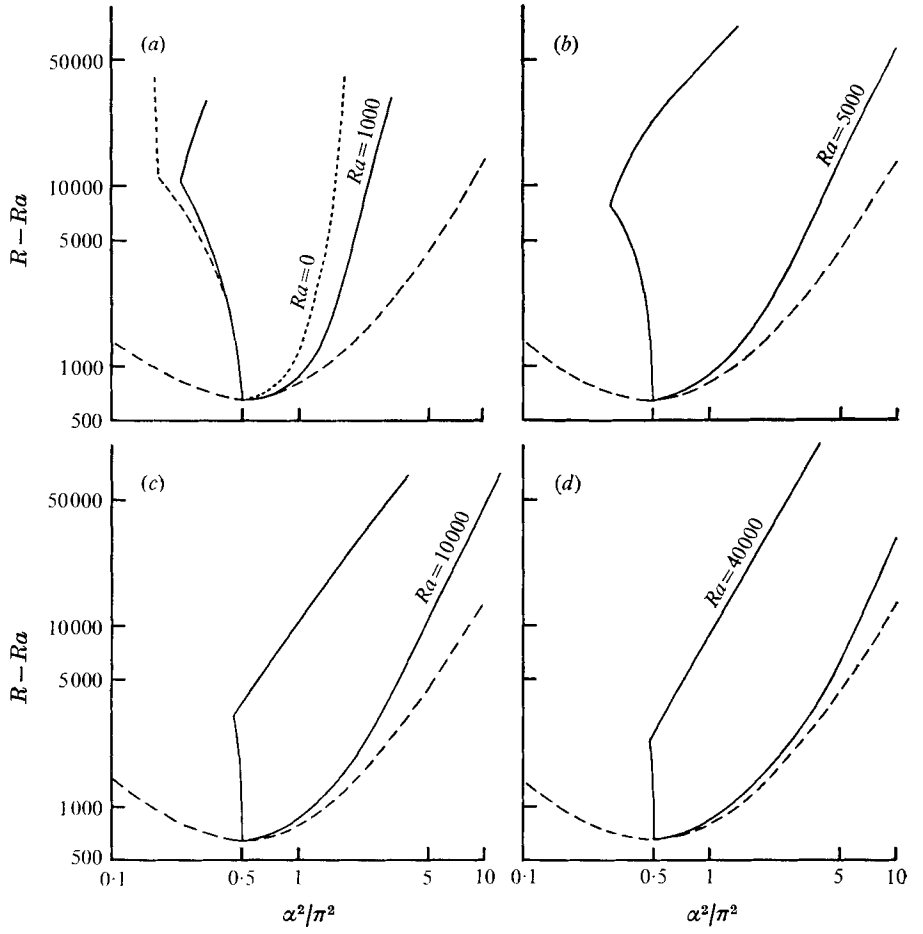

FIGURE 5. Regions of stable rolls for (*a*) $Ra = 0, 10^3$, (*b*) $Ra = 5 \times 10^3$, (*c*) $Ra = 10^4$, (*d*) $Ra = 4 \times 10^4$. – – –, marginal stability.

In figures 5(*a*)–(*d*) the regions of stable roll solutions are plotted so that this tendency may be more easily seen. The stability boundary for disturbances at a slight inclination to the original roll is seen here for $\alpha^2 < \frac{1}{2}\pi^2$ when R is less than some value that varies with Ra. For large $R - R_c$, this type of instability is unimportant, and we need not be concerned with it in determining the most stable wavenumber. The important observation that the region of stable rolls for singly diffusive convection ($Ra = 0$) shows no tendency for large wavenumbers to be preferred is clear here. The doubly diffusive instability is thus quite different from Bénard convection: the wavelength of steady flow should be much smaller at large values of Ra and of R/R_c than that at marginal stability. In fact, for large enough R/R_c the wavenumber $\alpha = \pi/\sqrt{2}$ predicted by linear stability theory at marginal stability is unstable.

One of the most important results of this investigation is shown in figure 6, in which smoothed curves have been drawn through the points corresponding to maximum Nu^s and maximum stability for the representative case $Ra = 4 \times 10^4$.

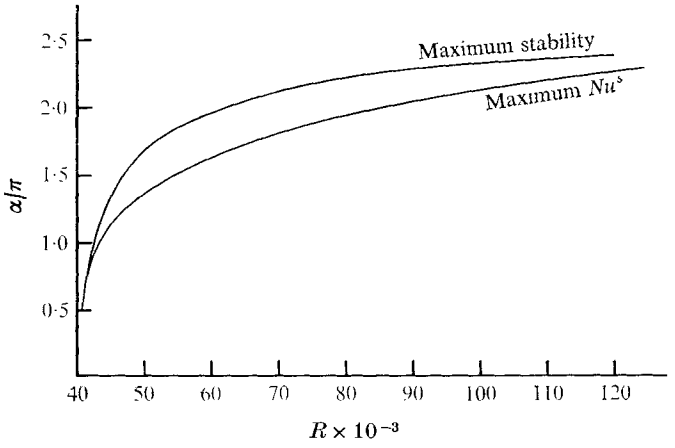

FIGURE 6. Comparison of the wavenumbers corresponding to maximum Nu^s and maximum stability for $Ra = 4 \times 10^4$.

In the preceding discussion we have noted that the 'most stable' wavenumber behaves in a manner very similar to that of the wavenumber at which Nu^s is maximized as R and Ra are varied. Here we make specific comparisons of these two wavenumbers. The correspondence, although not exact, is quite striking. It indicates that the stability of steady finite amplitude solutions is definitely related to their ability to transport salt across the layer. It also lends further support to the hypothesis that the flow prefers the wavelength that maximizes the rate of salt transport across the layer and that the maximum-transport hypothesis can be used as an approximate criterion for stability. Such a conclusion is difficult to make in a theoretical analysis of the singly diffusive problem because the range of wavenumbers does not vary much from that at marginal stability, but the wavenumbers in this analysis of the doubly diffusive problem cover a much wider range and thus allow a better comparison to be made.

5. Discussion

Several important results of the foregoing analysis will be summarized here. Although the model problem treated in this work has been the salt finger instability, the same type of analysis is applicable to other doubly diffusive instabilities, and similar results are anticipated. In particular, a fluid of small Prandtl number subjected to a destabilizing angular momentum distribution and a stabilizing temperature gradient, as in the work of Goldreich & Schubert, should show the same qualitative features as does the salt finger instability.

The central theme of the present investigation has been an elucidation of the problem of wavelength selection in the doubly diffusive instability. Because of the drastic change of horizontal scale which the salt finger instability undergoes for R much greater than its critical value, this problem is ideally suited for a treatment of wavelength selection. It has been shown here that the small horizontal wavelength associated with salt fingers may be explained as being due to the instability of modes with longer wavelengths. It was shown that, in addition to the observation that the preferred wavenumber $\tilde{\alpha}$ increases with increasing

$R-R_c$, $\tilde{\alpha}$ also increases as Ra increases for a constant value of R/R_c. For large values of $R-R_c$, $\tilde{\alpha}$ seems to approach an asymptotic limit that is a function of Ra, but this limiting dependence could not be determined here. The power law for the salt Nusselt number obtained appears to be approaching one of the form

$$RNu^s = c(R-Ra)^{\frac{4}{3}}$$

for larger values of R and Ra, although the present work may not have included large enough values of R and Ra for a definite asymptotic limit to have been reached. It is of interest to compare this result with Turner's (1967) experimental work. He found that the salt buoyancy flux obeys the power law

$$\beta F_s = (\beta\Delta S)^{\frac{4}{3}}(g\nu)^{\frac{1}{3}} f\left(\frac{\alpha\Delta T}{\beta\Delta S}, \frac{\nu}{\kappa_T}, \frac{\nu}{\kappa_S}\right) = C(\beta\Delta S)^{\frac{4}{3}};$$

here f is a slowly decreasing function of $\alpha\Delta T/\beta\Delta S$. Using the power law derived here, the buoyancy flux may be written as

$$\beta F_s = c\left(\frac{g\kappa_S^2}{\nu}\right)^{\frac{1}{3}}(\beta\Delta S)^{\frac{4}{3}}\left(1-\frac{\tau\alpha\Delta T}{\beta\Delta S}\right)^{\frac{4}{3}}.$$

The factor $(1-\tau\alpha\Delta T/\beta\Delta S)^{\frac{4}{3}}$ is a slowly decreasing function of $\alpha\Delta T/\beta\Delta S$. The value of $c \sim 0{\cdot}3$ leads to a value for C about one order of magnitude smaller than that obtained by Turner. As was pointed out in the introduction, the problem treated here has boundary conditions different from those of Turner's laboratory experiments and does not include the effects of three-dimensional motion. Turner's experiments were also made with values of R and Ra considerably larger than those treated here, so that the motion was probably a turbulent, rather than a laminar, one. With these facts in mind, the comparison of these functional forms seems to indicate that the physical processes important in doubly diffusive instabilities have been included in this model.

Perhaps the most general result of this work is concerned with the comparison made between the wavelength that leads to the maximum salt flux and that which is the most stable to perturbations. Although the conclusion that the most stable mode is to be preferred by the flow is not a rigorous one, the most stable mode lies near the centre of the wave band of stable modes and lends itself to comparison with other relevant wavelengths in the problem. The fact that the mode which maximizes the salt flux always lies within the wave band of stable modes suggests that the stability of a particular flow is related to its ability to transport salt across the layer. This is a concept put forth by Busse (1967) and, as he pointed out, is physically understandable because of the requirement of the stability of the boundary layers at the top and bottom of the fluid layer. In contrast tc Busse's findings for rigid boundaries, this analysis shows that the region of stable rolls does not close at any value of $R-R_c$ for free boundaries. Free boundaries allow the flow to extend closer to the boundaries since the no-slip condition there need not be satisfied, and thus allow a larger transport of the destabilizing component of the fluid. Thus, for any value of $R-R_c$, there is a non-vanishing band of wavelengths of the motion that lead to a value of the Nusselt number large enough to give stability.

The author would like to thank Professor F. H. Busse for many helpful suggestions and comments both prior to and during the present investigation. This work constitutes a portion of the author's Ph.D. dissertation submitted to the Department of Planetary and Space Science at UCLA and was supported by the National Science Foundation, NSF Grant GA-31247.

REFERENCES

BAINES, P. G. & GILL, A. E. 1969 *J. Fluid Mech.* **37**, 289.

BULIRSCH, R. & STOER, J. 1966 *Numerische Mathematik*, **8**, 1.

BUSSE, F. H. 1967 *J. Math. Phys.* **46**, 140.

BUSSE, F. H. 1971 In *Instability of Continuous Systems* (ed. H. Leipholz). Springer.

FRAZER, R. A., DUNCAN, W. J. & COLLAR, A. R. 1952 *Elementary Matrices*. Cambridge University Press.

GOLDREICH, P. & SCHUBERT, G. 1967 *Astroph. J.* **150**, 571.

LORTZ, D. 1968 *Z. angew. Math. Phys.* **19**, 682.

MALKUS, W. V. R. 1954 *Proc. Roy. Soc.* A **225**, 185, 196.

NIELD, D. A. 1967 *J. Fluid Mech.* **29**, 545.

RALSTON, A. & WILF, H. S. 1960 *Mathematical Methods for Digital Computers*. Wiley.

SCHLÜTER, A., LORTZ, D. & BUSSE, F. H. 1965 *J. Fluid Mech.* **23**, 129.

SHIRTCLIFFE, T. G. L. & TURNER, J. S. 1970 *J. Fluid Mech.* **41**, 707.

STERN, M. 1960 *Tellus*, **12**, 172.

STERN, M. & TURNER, J. S. 1969 *Deep Sea Res.* **16**, 497.

TURNER, J. S. 1967 *Deep Sea Res.* **14**, 599.

VERONIS, G. 1966 *J. Fluid Mech.* **26**, 49.

WALIN, G. 1964 *Tellus*, **16**, 389.

YIH, C.-S. 1970 *Phys. Fluids*, **13**, 2907.